Computational Condensed Matter 6 (2016) 18–23

Contents lists available at ScienceDirect

Computational Condensed Matter

journal homepage: http://ees.elsevier.com/cocom/default.asp

Regular article

Calculated electronic, transport, and bulk properties of zinc-blende zinc sulphide (zb-ZnS)

B. Khamala [a, b], L. Franklin [a], Y. Malozovsky [a], A. Stewart [a, c], H. Saleem [a], D. Bagayoko [a, *]

[a] Department of Physics, Southern University and A&M College, Baton Rouge, LA 70813, USA
[b] Computational Science Program, The University of Texas at El Paso, El Paso, TX 79968, USA
[c] Department of Mathematics & Computer Science, Allen University, Columbia, SC 29204, USA

ARTICLE INFO

Article history:
Received 12 November 2015
Accepted 5 December 2015
Available online 5 January 2016

ABSTRACT

We present the results from *ab initio*, self-consistent, local density approximation (LDA) calculations of electronic and related properties of zinc-blende zinc sulphide (zb-ZnS). We employed the Ceperley and Alder LDA potential and the linear combination of atomic orbital (LCAO) formalism. Our calculations are non-relativistic. The implementation of the LCAO formalism followed the Bagayoko, Zhao, and Williams (BZW) method, as enhanced by Ekuma and Franklin (BZW-EF). The BZW-EF method includes a methodical search for the optimal basis set that yields the minima of the occupied energies. This search entails increasing the size of the basis set and related modifications of angular symmetry and of radial features. Our calculated, direct band gap of 3.725 eV, at the Γ point, is in excellent agreement with experiment. We have also calculated the total (DOS) and partial (pDOS) densities of states, electron and hole effective masses and the bulk modulus that agree very well with available, corresponding experimental results.

1. Introduction

Zinc sulfide (ZnS) is an important semiconductor material with exceptional physical and chemical properties. It has a number of potential applications in optical coatings, solid-state solar window layers, electro optic modulators, photoconductors, field effect transistors, optical sensors, photo catalysts, and other light emitting materials. Zinc sulphide exists in two crystal structures, zinc-blende (zb-ZnS) and wurtzite (w-ZnS). Typically, the stable phase structure at room temperature is zinc blende [1]. Table 1 below shows a list of some calculated and experimental band gaps for zb-ZnS. A photoluminescence (PL) study of properties of zb-ZnS thin films led to a room temperature (320 K) band gap of 3.723 eV [2]. These authors [2] utilized metalorganic molecular beam epitaxy (MOMBE) and chemical beam epitaxy (CBE), between 1.6 and 320 K, to grow their samples. At 10 K, the PL spectrum showed peak energies between 3.73 eV and 3.82 eV. The peak energies at 3.80 eV and 3.795 eV were attributed [2] to light hole and heavy hole splitting as a result of elastic strain due to the difference in thermal expansion between ZnS and gallium arsenide (GaAs). These values were in good agreement with those of Taguchi et al. [3] who obtained 3.801 eV at 4.2 K, and with the findings of Abounadi et al. [4]. Taguchi et al. [3] grew ZnS thin films by metalorganic chemical vapor deposition (MOCVD), while Abounadi et al. [4] used low temperature reflectivity measurements to obtain peaks between 3.799 eV and 3.8005 eV, which largely depended on substrate orientation and temperature increments.

Trans et al. noted the difficulty in determining the band gap (E_g) for bulk ZnS at room temperature, due to a lack of commercially available bulk ZnS of high quality [2]. These reported band gap values for bulk ZnS varied from 3.56 eV to 3.764 eV. The absorption techniques gave a lower value of 3.56 eV partly due to the difficulties in the precise determination of location of the band edge and the method of analysis or interpretation of optical data. Cardona et al. [5] and Thesis [6], in their reflectivity and wavelength modulated reflectivity measurements, obtained band gap values of 3.74 eV and 3.76 eV, respectively, for bulk ZnS. A room temperature band gap of 3.723 ± 0.001 eV [2] was obtained by using MOMBE and CBE techniques. This band gap is close to 3.715 eV [7] and smaller than 3.80 eV [4]. Ahmed et al. obtained band gaps of 3.5 eV–3.7 eV [8] for samples grown by chemical co-precipitation. Their measurement techniques were X-ray Diffraction (XRD) and Scanning Electron Microscopy (SEM). Mir [9], in his study of the

* Corresponding author.
E-mail address: bagayoko@aol.com (D. Bagayoko).

http://dx.doi.org/10.1016/j.cocom.2015.12.001

Table 1
Calculated band gaps of zb-ZnS versus experimental ones for zb-ZnS.

Computational formalism and method	Potentials (DFT and others)	E_g (eV)
Pseudopotential- Plane wave	LDA	2.37[b]
Pseudopotential- Plane wave	LDA	1.65[f]
Pseudopotential- Plane wave	LDA	1.84[l]
Pseudopotential- Plane wave	LDA	1.84[g]
Pseudopotential-Plane wave	LDA	3.55[p]
LMTO-ASA	LDA	1.85[d]
Pseudopotential- Plane wave	GGA	2.03[f]
Pseudopotential- Plane wave	LDA + GW	3.98[b]
Pseudopotential- Plane wave	LDA + GW	3.64[f]
Pseudopotential- Plane wave	GGA + GW	3.27[f]
Pseudopotential- Plane wave	mBJLDA	3.66[g]
FP-(L)APW + LO	mBJ + LDA latt. (5.308 Å)	3.85[h]
FP-(L)APW + LO	mBJ + GGA latt. (5.452 Å)	3.55[h]
Hybridized density Functional	HSE03	3.49[g]
FP-(L)APW + LO	mBJ latt. $_{avg}$ (5.380 Å)	3.70[c,h]
Linear Combination of Atomic Orbitals (LCAO)	LDA	3.81[n]
Linear Combination of Gaussian Orbitals (LCGO)	LDA	2.26[m]
Orthogonalized Linear Combination of Atomic Orbitals (OLCAO)	LDA	2.34[r]
Experiment		
Experimental	Photoluminescence measurements at room temp.	3.723 ± 0.001[a]
	Reflectivity Measurements at low temp growths (at 300 °C)	3.80[i]
	At room temp.	3.70[j]
	Thermal evaporation method (At 1100 °C then cooled to room temp)	3.50–3.70[c,k]
	Photoluminescence and Absorption spectroscopy at room temp.	3.74[e]

[a] Reference [2].
[b] Reference [10].
[c] Reference [8].
[d] Reference [11].
[e] Reference [6].
[f] Reference [12].
[g] Reference [13].
[h] Reference [14].
[i] Reference [4].
[j] Reference [9].
[k] Reference [15].
[l] Reference [16].
[m] Reference [17].
[p] Reference [18].
[n] Reference [19].
[r] Reference [20].

optical properties of ZnS nanocrystals, used the UV–Vis spectroscopy approach. He determined the band gap to be 3.7 eV at room temperature. From the preceding, it appears that various experimental studies basically agree on the band gap of zb-ZnS. This gap is about 3.8 eV at very low temperature and approximately 3.72 eV at room temperature. The relatively small uncertainty for photoluminescence measurements of the band gap, as compared to optical absorption ones, led to the preference for 3.72 eV. This agreement between experimental works is in contrast to the case for ab-initio, theoretical calculations of electronic properties (including the band gap) of zb-ZnS.

The theoretical underestimation of the band gap for ZnS has been ascribed to the inadequacies of density-functional potentials for the description of semiconductors [21,22]. The band gap values reported by some previous local density approximation calculations, range from 1.65 to 2.37 eV [10–12]. Weidong et al. [12] constructed pseudopotentials and then varied the cut-off radius until a good approximation was found. Zakharov et al. [10] also used the pseudopotential method and adjusted the d-character in the valence-band maximum (VBM) by adding a short-range attractive potential in non-local d channel of the Zn pseudopotential to fit the experimental position. They obtained $E_g = 2.31$ eV, though close but smaller than their previous result of 2.37 eV for zb-ZnS. They concluded that LDA underestimated the band gap by 30–40%. With the Green function and the screened coulomb interaction, (GW), they obtained 3.98 eV and 4.03 eV for zb-ZnS and w-ZnS, respectively. Weidong et al. [12] obtained $E_g = 2.03$ eV with a generalized gradient approximation (GGA) potential and 3.27 eV with (GGA + GW).

Willatzen et al. [23,24] in their "Luttinger Parameters, spin splitting", worked on generating the corrected band parameters for a number of semiconductors. Other calculations reported [11,25] values for the band gap that cover a wide range of values, from 1.80 eV to 2.20 eV. The linear muffin-tin orbital (LMTO) and linear muffin-tin orbital atomic-sphere approximation (LMTO-ASA) computational methods [11] obtained a very small band gap value of 1.85eV.

From the preceding, it appears that previous theoretical results mostly disagree with each other and with experimental ones. The above discrepancies are key motivations for our work. We used the Bagayoko, Zhao, and Williams (BZW) method, as enhanced by Ekuma and Franklin (BZW-EF) in attaining highly accurate results.

Other properties investigated included the effective masses and the bulk modulus from the total energy calculations. Wang [17] calculated effective hole masses in the [100] and [111] directions, where we note the considerable anisotropy for the two directions. A previous local density approximation (LDA) result for the electron effective mass [22] of 0.141 m_o is 23% lower than the experimental

value [17] of 0.184 m_o.

The bulk modulus is a measure of the strength and hardness of many materials [26]. Materials with the largest bulk moduli are usually expected to be the hardest ones [26]. ZnS has the largest overall elastic stiffness and bulk modulus among II-VI semiconductors [27]. The elastic stiffness coefficients are essential for many applications in solids such as internal strain, thermoelastic stress and load deflection [28]. Imad [27] obtained a bulk modulus for ZnS to be 78 GPa. Cohen [29] obtained an empirical expression for the bulk modulus based on the nearest-neighbor distance. His calculated value of 90 GPa deviates by 14.4% from the experimental value of 77 GPa [27]. Lam et al. [30] obtained an expression for the bulk modulus for ZnS using the total energy method with acceptable results.

In this paper, we present ab-initio calculations of electronic, transport and bulk properties of zb-ZnS. We used the LCAO formalism of solving a pertinent system of equations self consistently [31–34]. The details of the method and the computations will be discussed in section II below. The results and discussions of our self-consistent calculations are presented in sections III and IV, respectively. A conclusion is given in section V.

2. Methods and computational details

We utilized a program package developed and refined over decades [35,36]. We employed the room temperature, experimental lattice constant of 5.409 Å [11]. Our calculations began with LCAO, self-consistent calculations of the electronic energy levels of the ionic species that are present in the system under study. For zb-ZnS, these species are Zn^{2+} and S^{2-}; the calculations for the neutral atoms (Zn and S) were utilized in preliminary investigations of the solid state. The results from the preliminary calculations were employed to compute charge transfer, between Zn and S sites in the solid, which was found to be approximately two electrons from zinc to sulphur. Consequently, ab-initio, self-consistent calculations were performed for Zn^{2+} and S^{2-} ions in order to obtain the "'atomic"' basis sets to be employed in the actual solid state calculations.

Our self-consistent solid state calculations, as per the BZW-EF method [33,37–40], began with a small basis (MB) set, i.e., one that is enough to account for all the electrons in the system. As shown in Table 2, Calculation II utilizes a basis set of Calculation I as augmented by one additional orbital representing a higher energy level in the ionic species in the system. For a given principal quantum number, the applicable polarization orbitals (p, d, and f) are added, in that order, before the corresponding s orbital. This approach recognizes the fact that in systems varying from binary molecules to solids, the distribution of the cloud of valence electrons is expected to deviate from spherical symmetry.

The occupied energies from Calculations I and II are compared numerically and graphically. They are generally found to be different, with some occupied energies from Calculation II being lower than corresponding ones from Calculation I. The above lowering of some occupied energies from Calculation II indicates that the first basis set is not complete in size, angular symmetry, or radial functions for the description of the ground state. Calculation III is performed with a basis set including that of Calculation II as augmented with an orbital representing the next appropriate excited levels of the ionic species in the system. This process of augmenting the basis set and of carrying out self-consistent calculations continues until the occupied energies from a calculation, i.e., N, are the same as those of Calculation $(N+1)$ and $(N+2)$, within computational uncertainties of 5 meV. As explained elsewhere [41–43] and below, the outputs of Calculation N provide the physical description of the material under study. The basis set for this calculation is referred to as the optimal basis set [41–43], i.e., the smallest basis set that leads to the absolute minima of all the occupied energies. With the BZW-EF method, we actually verify the completeness of the basis set vis à vis the description of the occupied states, instead of assuming it.

The fundamentally ground state nature of density functional theory indicates that the above BZW-EF method, at a minimum, is a viable alternative to others that utilize a single trial basis set. The actual size of the optimal basis set naturally depends on the types of functions, with plane wave procedures entailing many more basis functions than those utilizing localized, exponential, or Gaussian functions. In Calculation $(N+1)$ and others with larger basis sets that include the optimal one, the charge density and the occupied energies do not change from their values obtained with Calculation N [41–43]. Successive calculations with larger basis sets that contain the optimal one generate increasing numbers of eigenvalues, by virtue of the fundamental theorem of algebra, with some unoccupied ones, for a given calculation, being lower than their corresponding ones in the calculation immediately preceding it, as per the Rayleigh theorem. This mathematical artifact is the non-trivial basis set and variational effect [31,44,45] totally avoided by the BZW-EF method as explained below.

The Rayleigh theorem states that when an eigenvalue equation is solved with two basis sets containing n and $(n+1)$ basis functions, respectively, with the smaller basis set totally included in the larger one, then the ordered eigenvalues (from the lowest to the highest) obtained with $(n+1)$ functions are lower than or equal to their corresponding ones obtained with n functions. In the implementation of the BZW-EF method, we avoid the above basis set and variational effect by selecting the outputs from the calculation with the optimal basis set; larger basis sets that contain the optimal one, some unoccupied energies, often including the lowest laying ones, are lowered further by this effect while the charge density and the Hamiltonian do not change. These larger basis sets that contain the optimal one are over complete for the description of the ground state.

Computational details germane to the replication of our work follow. ZnS possesses a cubic lattice in the space group F4-3m. There are four asymmetric units in its unit cell. The atomic positions are as follows: Zn: 0.25, 0.25, 0.25; S: 0, 0, 0. The self-consistent computations were performed at a lattice constant of

Table 2
Successive LDA BZW-EF Calculations (I–VI) for zb-ZnS. The room temperature experimental lattice constant utilized was 5.409 Å. **Calculation III** led to the absolute minima of all the occupied energies; the superscript zero indicates orbital representing unoccupied atomic levels.

Calculation no.	Valence functions for Zn^{2+}	Valence functions for S^{2-}	Total Valence functions	Band Gap (in eV)
1	$3s^23p^63d^{10}4s^0$	$2s^22p^63s^23p^6$	36	3.316
2	$3s^23p^63d^{10}4s^04p^0$	$2s^22p^63s^23p^6$	42	3.796
3	$\mathbf{3s^23p^63d^{10}4s^04p^04d^0}$	$\mathbf{2s^22p^63s^23p^6}$	**52**	**3.725**
4	$3s^23p^63d^{10}4s^04p^04d^0$	$2s^22p^63s^23p^63d^0$	62	3.723
5	$3s^23p^63d^{10}4s^04p^04d^05S^0$	$2s^22p^63s^23p^63d^0$	64	2.434
6	$3s^23p^63d^{10}4s^04p^04d^05S^0$	$2s^22p^63s^23p^63d^04S^0$	66	2.306

5.409 Å, for room temperature [10,11]. We employed a mesh of 44 k-points, with proper weights, in the irreducible Brillouin zone. Our criterion for self-consistency of the iterative solutions of the Kohn–Sham Equation rested on the convergence of the potential to a difference around 10^{-5} between two consecutive iterations. Approximately 60 iterations were needed to reach self-consistency for the Kohn–Sham equation. The computational error for the valence charge was 0.000007 for 34 electrons.

3. Results

Results of our computations are given in Figs. 1–2 and Tables 1–5. We discuss the electronic structure in subsection III. 1. Details on our density of states (DOS), partial densities of states, effective masses, and the total energy and bulk modulus are in subsections III.2, III.3, and III.4, respectively.

3.1. Electronic energy bands and band gap of zb-ZnS

Table 2 lists the self-consistent calculations for zb-ZnS, with different trial basis sets. The resulting band gaps cover a wide range of values, from 2.31 eV to 3.80 eV Fig. 1 shows the bands from self-consistent Calculations III and IV. Calculations V and VI led to the same occupied energies as obtained in Calculations III and IV. While Calculations III and IV led to the same unoccupied energies up to 10 eV. Calculation V and VI produced some unoccupied energies lower than their corresponding ones from Calculation III, due to the basis set and variational effect. Consequently, Calculations V and VI yielded band gaps much smaller than that from Calculation III. The occupied bands obtained from Calculation III and IV, as shown in Fig. 1, are very similar to those of some previous LDA calculations [10–12]. The picture is drastically different for unoccupied energies as elaborated upon in the section on discussions.

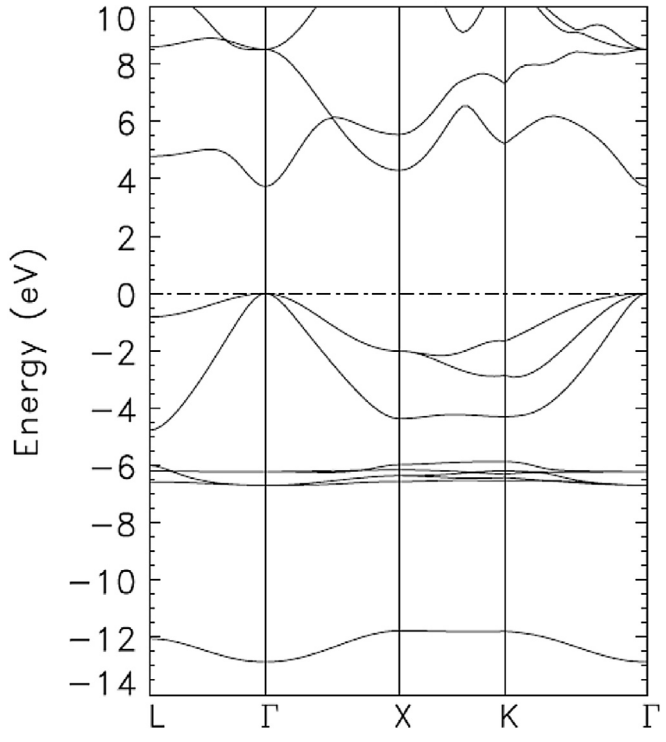

Fig. 1. Calculated band structure of zinc-blende zinc sulphide (zb-ZnS), as obtained from Calculations III (_) and IV (_ _), at the room temperature experimental lattice constant of 5.409 Å. The band gap is 3.73eV. For the shown bands (occupied and unoccupied), the results from Calculations III and IV are the same, within the computational uncertainties estimated at 0.002eV, as attested to by the perfect superposition. The Fermi energy (E_F) has been set to zero.

Fig. 1 shows that the top of the valence band is at the Γ point. Our lowest, calculated valence band energy of −12.86 eV, at Γ, is close to the −12.63 eV of Zakhorov et al. [10]. As shown in Fig. 3, the upper most group of valence bands are from zinc p and d, with smaller contributions from sulfur s and p. The hybridized bands around −6.5 eV are Zn d and S s and p.

Table 3 shows the eigenenergies along high symmetry points for zb-ZnS, as obtained from Calculation III with the room temperature experimental lattice constant of 5.409 Å. The content of this table is intended to enable detailed comparisons with some future experimental findings. The total width of the valence bands is 12.857 eV. The valence bands are split into three groups separated by 1 eV and 5 eV, respectively. As per the pDOS in Fig. 3, the lower lying group consists mostly of Zn-p, Zn-d and some contributions from S-s and S-p. The middle group consists of highly hybridized Zn-d, S-s, and S-p while the upper group is dominated by the Zn-p, Zn-d, and S-s with some S-p. The width of this uppermost group of the valence bands is 4.77 eV. Those of the middle and lowest lying valence bands are 0.87 eV and 1.07 eV, respectively. These widths are much closer to experimental results [10].

3.2. Densities of states

Figs. 2 and 3 exhibit the total (DOS) and partial (pDOS) densities of states, respectively. From our calculated DOS (see Fig. 2), it can be inferred that the onset of absorption is quite sharp and it starts at about 3.73 eV. In the low laying conduction bands, sharp peaks appear at 5.86 eV, 7.43 eV, and 9.30 eV. For the valence bands DOS, we calculated peaks at −11.80 eV, −6.56 eV, −6.19 eV, −4.29 eV, −2.69 eV and −1.99 eV. These positions of the peaks are nearly the same as corresponding experimental ones, from x-ray spectroscopy [1], as shown Table 5.

3.3. Effective mass

The effective mass is one of the main factors determining the transport properties of materials. The effective mass is a measure of the curvature of the calculated bands. We calculated the effective masses of the n-type carriers of ZnS using the bands in Fig. 1, Calculation III. We obtained 0.154 m_o, 0.174 m_o, 0.162 m_o in the Γ to L, Γ to X, and Γ to K directions, respectively. Our value of 0.174 m_o, from Γ to X, agrees with the measured one of 0.178–0.188 ± 0.005 m_o [46].

We also calculated hole-effective masses at the top of the valence band along the Γ to L, Γ to X, and Γ to K directions. We found heavy hole effective masses of 1.550 m_0, 1.772 m_0, and 1.066 m_0 from Γ to L, Γ to X, and Γ to K, respectively. Our calculated light hole effective masses from Γ to L, 0.166 m_0, is in excellent agreement with the experimental value of 0.169 [47]. Similarly, our light hole effective mass from Γ to X of 0.211 m_0 is close to the experimental finding of 0.230 m_0 [17]. The agreement between calculated and measured effective masses indicates an accurate determination of the curvature of the bands in vicinity of the Γ point.

3.4. Total energy and bulk modulus

The calculated total energies for zb-ZnS, at different lattice constants, are shown in Fig. 4. The calculated equilibrium lattice constant of zb-ZnS, i.e., the value at the minimum of the total energy curve, is 5.396 Å. This value is in excellent agreement with the experimentally measured lattice constant of 5.409 Å [10]. The calculated bulk modulus of zb-ZnS, from the total energy curve in Fig. 4, is 78 GPa, which also agrees well with the measured values of

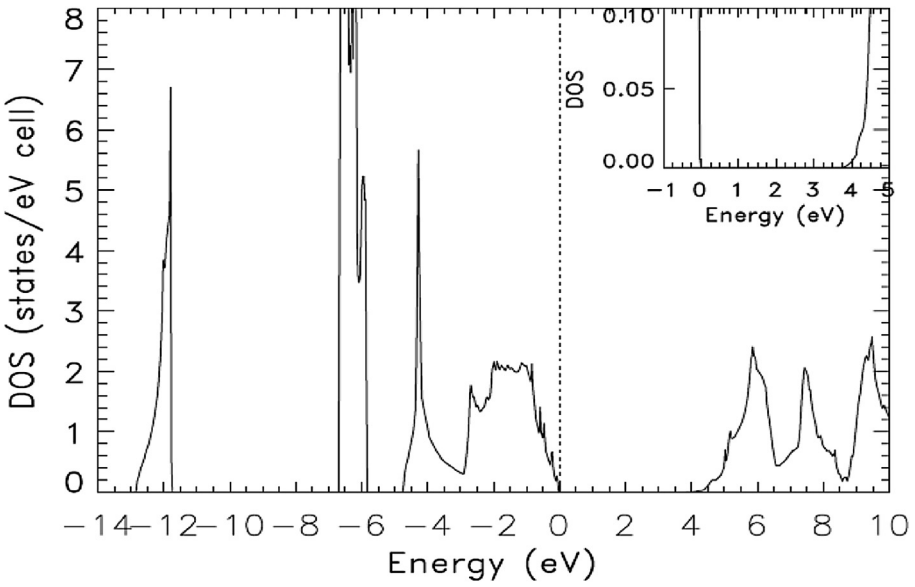

Fig. 2. Calculated total density of states (DOS) of zb-ZnS, at the lattice constant of 5.409 Å, as obtained with the bands from Calculation III.

Table 3
Eigenvalues (eV), along high symmetry points, for zb-ZnS, as obtained from calculation III, with the experimental lattice constant of 5.409 Å. The Fermi energy is set to zero.

L-point	Γ-point	X-point	K-point	Γ-point
10.411	8.515	13.249	11.605	8.515
8.601	8.515	12.256	11.479	8.515
8.601	8.515	5.545	7.323	8.515
4.782	**3.725**	**4.291**	**5.226**	**3.725**
−0.820	0.000	−2.013	−1.668	0.000
−0.820	0.000	−2.013	−2.857	0.000
−4.770	0.000	−4.365	−4.302	0.000
−6.007	−6.217	−5.975	−5.874	−6.217
−6.197	−6.217	−6.162	−6.193	−6.217
−6.197	−6.697	−6.364	−6.304	−6.697
−6.579	−6.697	−6.364	−6.426	−6.697
−6.579	−6.697	−6.569	−6.539	−6.697
−12.046	−12.857	−11.776	−11.794	−12.857

Table 4
Effective masses (in units of the free electron-mass, m_o): M_e for the effective electron mass at the bottom of the conduction band; $M_{hh,}$ and M_{lh} are the heavy and light hole effective masses, respectively, at the top the valence band.

	Present	Theo[a]	Theo[b]	Expt[c]	Expt[d]
M_e (Γ-L)	0.154	0.142			
M_e (Γ-X)	0.174	0.141		0.184[b,c]	0.178 ± 0.005
M_e (Γ-K)	0.162	0.141			
M_{hh} (Γ-L)	1.550				
M_{hh} (Γ-X)	1.772	0.602	0.121		
M_{hh} (Γ-K)	1.066	3.071, 0.602		1.121	
M_{lh} (Γ-K)	0.833	1.297	1.652		
M_{lh}(Γ- L)	0.166	0.119	0.153	0.169	
M_{lh}(Γ-X)	0.211	0.126		0.230[b]	
M_{lh} (Γ-K)	0.192	0.151	0.198		

[a] Reference [22].
[b] Reference [17].
[c] Reference [47].
[d] Reference [46].

78 GPa [27], 77 GPa [27,29,30], and 75 GPa [48].

Table 5
Comparison of calculated and experimental peaks in the total density of states. The labels (H_{1T}, I_2, I_1, S_1, H_{1B}, P_{11}, H_{IIB}, E_{11}, E_{11I}, H_{IIIT}, P_{11I}) are in Fig. 14 of Reference [1].

	H_{1T}	I_2	I_1	P_{11}	H_{IIB}	P_{11I}
Present work	0.75	2.00	2.50	4.50	6.25	12.25
Expt	0.80	2.00	2.60	4.90	5.90	12.40

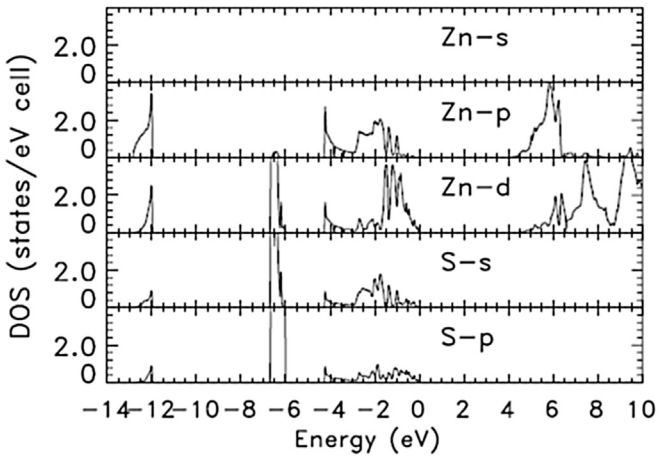

Fig. 3. Calculated, partial densities of states (pDOS) of zb-ZnS, at the lattice constant of 5.409 Å, as obtained with the bands from Calculation III.

4. Discussions

The physical origin of the changes in the band gap as the basis set increases towards the optimal one stems from a better representation of the electronic cloud by larger basis sets. This increase leads not only to that of the size of the basis set (and the dimension of the Hamiltonian), but also to an enrichment of the radial orbitals and of the angular symmetries. The three changes directly enhance the variational freedom for an adequate representation of the redistribution of the electronic cloud in the system under study as compared to those around isolated atomic or ionic species. The

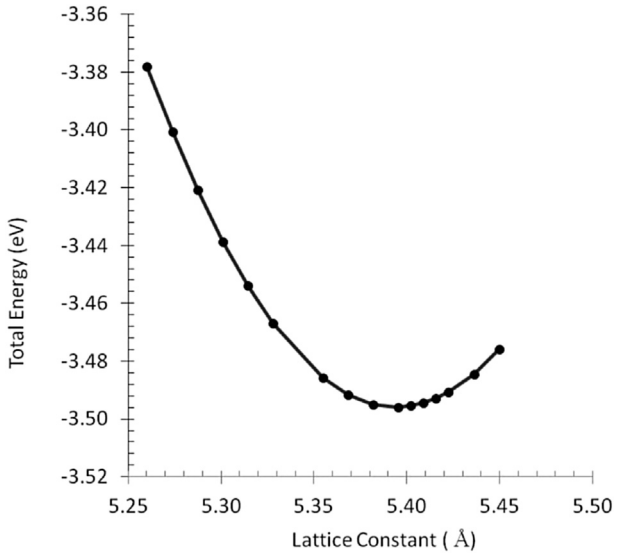

Fig. 4. The calculated, total energy of zb-ZnS versus the lattice constant. The minimum total energy is located at the equilibrium lattice constant of 5.396 Å.

critical importance of the enhanced variational freedom rests on the derivation of DFT (or LDA [41–43].

As explained above in the section on our method, Calculations III, IV, and V, as well as others with larger basis sets, led to the same occupied energies. Calculation III, as identified by the BZW-EF method, is the one providing the correct DFT description of zb-ZnS; the corresponding basis set is the optimal one. This double verification (by IV and V) of the attainment of the absolute minima of the occupied energies led to that conclusion. Calculations III and IV led to the same low-lying, unoccupied energies, up to 10eV, as shown in Fig. 1. The Rayleigh theorem is integral to the BZW-EF method. It provides the mathematical reason for avoiding basis sets much larger than the optimal one, i.e., that of Calculation III. We underscore [41–43] the fact that the iterative process, irrespective of its degree of convergence, cannot correct any deficiency in the angular symmetry of the basis set [missing polarization functions or a spherical symmetry unnecessarily imposed on valence electrons].

The above features of the BZW-EF method explain the reasons that we obtained results in agreement with experiment. The method strictly adheres to necessary conditions for DFT eigenvalues to describe real systems [43]. None of the other calculations cited in this work did so, to our knowledge, as they mostly used a single basis set, or different basis sets that were not embedded.

5. Summary and conclusion

We have performed ab-initio, self-consistent calculations of the electronic energy bands, densities of states (DOS), partial density of states (pDOS), effective masses, and the bulk modulus of zinc-blende zinc sulphide, using the BZW-EF method. Our calculated results for the band gap, effective masses, and the bulk modulus are in excellent agreement with corresponding experimental ones.

The above LDA BZW-EF results point to the capability of DFT to describe and to predict accurately the electronic and related properties of semiconductors. As such, DFT BZW-EF calculations are expected to inform and to guide the design and fabrication of semiconductor and nanostructure based devices.

Acknowledgments

This research was funded in part by the National Science Foundation (NSF) and the Louisiana Board of Regents, through LASIGMA [Award Nos. EPS- 1003897, NSF (2010-15)-RII-SUBR] and NSF HRD-1002541, the US Department of Energy – National, Nuclear Security Administration (NNSA) (Award No. DE-NA0001861), LaSPACE, and LONI-SUBR.

References

[1] L. Ley, R.A. Pollak, F.R. McFeely, S.P. Kowalezyk, D.A. Shirley, Phys. Rev. B 9 (2) (1974).
[2] T.K. Tran, W. Park, W. Tong, M.M. Kyi, B.K. Wagner, C. Summers, J. Appl. Phys. 81 (2803) (1997).
[3] T. Taguchi, T. Yokogawa, H. Yamashita, Solid State Commun. 49 (551) (1984).
[4] A. Abounadi, M. Di Blasio, D. Bouchara, J. Calas, M. Averous, O. Briot, N. Briot, T. Cloitre, R.L. Aulombard, B. Gil, Phys. Rev. B 50 (11667) (1994).
[5] M. Cardona, M. Weinstein, G.A. Wolff, Phys. Rev. (1965) 140.
[6] D. Thesis, Phys. Status Solid B 79 (1977).
[7] O. Kanehisa, M. Shiiki, M. Migita, H. Yamamoto, J. Cryst. Growth. 86 (1988) 367–371.
[8] A. Mushtaq, et al., Structural and Electrical properties of ZnS nanoparticles.
[9] F.A. Mir, Optoelectron. Biomed. Mater. 2 (2) (2010).
[10] O. Zakharov, A. Rubio, X. Blase, M.L. Cohen, S.G. Louie, Phys. Rev. B 50 (15) (1994).
[11] Bal K. Agrawal, P.S. Yadav, S. Agrawal, Phys. Rev. B 50 (1994).
[12] W. Luo, S. Ismail-Beigi, M.L. Cohen, S.G. Louie, Phys. Rev.B 66 (2002).
[13] F. Tran, P. Blaha, Phys. Rev. Lett. 102 (226401) (2009).
[14] J.A. Camargo, R. Baquero, Phys. Rev. B 86 (2012).
[15] B.Y. Geng, X.W. Liu, Q.B. Du, X.W. Wei, Structure and optical properties of periodically twinned ZnS nanowires, Appl. Phys. Lett. 88 (163104) (2006).
[16] J.L. Martins, N. Troullier, S.H. Wei, Phys. Rev. B 43 (2213) (1991).
[17] C.S. Wang, B.M. Klein, Phys. Rev. B 24 (1981).
[18] P. Schroer, P. Kruger, J. Pollmann, Phys. Rev. B 47 (6971) (1993).
[19] M.Z. Huang, W.Y. Ching, Phys. Chem. Solids 46 (977) (1985).
[20] M.Z. Huang, W.Y. Ching, Phys. Rev. B 47 (9449) (1993).
[21] L.J. Sham, M. Schuluter, Phys. Rev. Lett. 51 (1983).
[22] S. ZKarazhanov, L.L.Y. Voon, Ab-initio studies of band parameters of AIIIBv and AIIBVI zinc blende semiconductors 39, 2005.
[23] M. Willatzen, M. cardona, N.E. Christensen, Phys. Rev. B 50 (1994).
[24] M. Willatzen, M. cardona, N.E. Christensen, Phys. Rev. B 51 (1995).
[25] M. Kanemoto, et al., Chem. Soc. 92 (2401) (1996).
[26] E. Kim, C. Chen, Calculation of bulk modulus for highly anisotropic materials, Phys. Lett. A 326 (2004) 442–448.
[27] A. Imad, M.S. Gaith, The measurement of overall elastic stiffness and bulk modulus in solar photovoltaic devices, Jordan J. Mech. Industrial Eng. 4 (1) (2010) 55–60.
[28] M. Belge, H.H. Kart, T. Cagin, Mechanical and electronical properties of ZnS under pressure, JAMME 31 (1) (2008).
[29] M.L. Cohen, Phys. Rev. B 32 (12) (1985).
[30] Pui K. Lam, Marvin L. Cohen, G. Martinez, Analytic relation between bulk moduli and lattice constants, Phys. Rev. B 35 (17) (1987) 9190–9194.
[31] G.L. Zhao, D. Bagayoko, T.D. Williams, Phys. Rev. B 60 (1563) (1999).
[32] D. Bagayoko, L. Franklin, G.L. Zhao, Phys. Rev. B 76 (2007).
[33] C.E. Ekuma, L. Franklin, J.T. Wang, G.L. Zhao, D. Bagayoko, Can. J. Phys. 89 (2011).
[34] D. Bagayoko, L. Franklin, Appl. Phys. 97 (2005).
[35] P.J. Feibelman, J.A. Appelbaum, D.R. Hamann, Phys. Rev. B 20 (1979).
[36] B.N. Harmon, W. Weber, D.R. Hamann, Phys. Rev. B 25 (1109) (1982).
[37] C.E. Ekuma, D. Bagayoko, Jpn. J. Appl. Phys. 50 (10103) (2011).
[38] C.E. Ekuma, M. Jarrel, J. Moreno, D. Bagayoko, AIP Adv. 2 (1) (2012) 012189.
[39] I.H. Nwigboji, J.I. Ejembi, Y. Malozovsky, B. Khamala, L. Franklin, G.L. Zhao, C.E. Ekuma, D. Bagayoko, Mater. Chem. Phys. 157 (2015) 80–86.
[40] A. Stewart, D. Hart, B. Khamala, Y. Malozovsky, D. Bagayoko, J. Adv. Phys 9 (1) (2015).
[41] C.E. Ekuma, M. Jarell, J. Moreno, G.L. Zhao, D. Bagayoko, Re-examining the electronic structure of germanium: a first principle Study, Phys. Lett. A 377 (34–37) (2013) 2172–2176.
[42] L. Franklin, G.L. Zhao, C.E. Ekuma, D. Bagayoko, Density functional theory description of electronic properties of wurtzite zinc oxide(w-ZnO), J. Phys. Chem. Solids 74 (729–736) (2013).
[43] D. Bagayoko, Understanding density functional theory(DFT) and completing it in practice, AIP Adv. 4 (127104) (2014).
[44] D. Bagayoko, G.L. Zhao, J.D. Fan, J.D. Wang, Phy. Condens. Matter 10 (5645) (1998).
[45] D. Bagayoko, L. Franklin, G.L. Zhao, H. Jin, Appl. Phys. 103 (2008).
[46] Y. Imanaka, N. Minra, Phys. Rev. B 50 (1994).
[47] O. Madelung and M. Schulz. Springer Verlag, Berlin, 1982. 22.
[48] S. Ves, U. Schwarz, N. Christen, K. Syassen, M. Cardona, Cubic ZnS under pressure: optical-absorption edge, phase transition, and calculated equation of state, Phys. Rev. B 42 (14) (1990) 9113–9118.